HIGH-PRECISION SIMS CHONDRULE OXYGEN ISOTOPE RATIOS FROM THE YAMATO 82094 UNGROUPED CARBONACEOUS CHONDRITE. T. J. Tenner[1], M. Kimura[2,3], and N.T. Kita[1]. [1]WiscSIMS, Dept. of Geoscience, Univ. of Wisconsin-Madison, USA (tenner@wisc.edu), [2]Faculty of Science, Ibaraki University, Mito, Japan, [3]National Institute of Polar Research, Tokyo, Japan.

Introduction: Yamato (Y) 82094 is a petrologic type 3.2 ungrouped carbonaceous chondrite [1]. The ratio of chondrules (78 vol. %) to matrix (11 vol. %) is high relative to CO, CV, and CR chondrites (45-60 vol. % chondrules vs. 30-50 vol. % matrix), but similar to CH and ordinary chondrites [2-4]. The average diameter of Y-82094 chondrules (330 μm; [1]) is distinct from those of CH (20 μm), CO (150 μm), CB (200 μm), CR (700 μm), and CV/CK (900 μm) chondrites, as well as chondrules from ordinary chondrites (450-550 μm) [5]. Y-82094 is dominated by type I ($Mg\#_{silicate} > 90$) chondrules (99.1 %); type II ($Mg\#_{silicate} < 90$) chondrules are rare (0.9 %), akin to other carbonaceous chondrites but different from LL3 chondrites, in which ~50 % are type II chondrules [6]. The Y-82094 bulk O-isotope ratio (δ^{17}O: –7.62 ‰; δ^{17}O: –4.52 ‰; [7]) is similar to that of other carbonaceous chondrites [8], but the O-isotope distribution among its chondrules is unknown. Here, we present O-isotope measurements of chondrules from Y-82094.

Samples & Methods: 34 chondrules were analyzed by SIMS, from NIPR sections 91-1, 91-4, 96-1, and 96-2. 27 are type I chondrules (15 porphyritic olivine-pyroxene, or POP; 8 Al-rich; 2 barred olivine; 1 porphyritic olivine, or PO; 1 porphyritic pyroxene) and 7 are type II (3 POP, 4 PO). In 22 of 34 chondrules, constituent low-Ca pyroxene Mg#'s define the chondrule Mg#, as Fe-Mg diffusion is slower in low-Ca pyroxene relative to olivine [9]; for the remaining type I chondrules, Mg#'s of olivine phenocrysts without FeO enrichment from thermal metamorphism define chondrule Mg#; for the remaining type II chondrules, Mg#'s of olivine phenocrysts without FeO-poor relict cores define chondrule Mg#. Electron microprobe techniques are described in [1]. Oxygen 3-isotope ratios were measured with the WiscSIMS Cameca IMS 1280, using multi-collector Faraday cups, as detailed in [6]. A primary Cs^+ ion beam (intensity: 2.6 nA) produced a 15 × 10 μm spot size. San Carlos olivine bracketing analyses correspond to δ^{18}O, δ^{17}O, and Δ^{17}O external reproducibilities (2SD) of 0.4, 0.5 and 0.5 ‰, respectively. 295 SIMS analyses of chondrule phenocrysts (olivine, pyroxene, plagioclase, spinel) were acquired (5 to 10 spots per chondrule). Homogeneous phenocryst O-isotope data per chondrule determine the averaged "host" value; phenocrysts with Δ^{17}O (= δ^{17}O – 0.52 × δ^{18}O) values differing by more than 0.7 ‰ (the 3SD external reproducibility) of the host chondrule Δ^{17}O were defined as relict grains.

Results and Discussion: Regardless of the types of phases measured, all chondrules have multiple homogeneous O-isotope data (2 to 9 per chondrule) that define their host value. Host chondrule O-isotope ratios plot on/near the PCM [10] line, between the CCAM [11] and Young & Russell [12] lines (Fig. 1). The distribution of host chondrule O-isotope ratios is similar to those from other carbonaceous chondrites [10,13-18], but different than that of LL3 chondrites [6] (Fig. 1). Type I chondrules in Y-82094 are ^{16}O-rich relative to type II

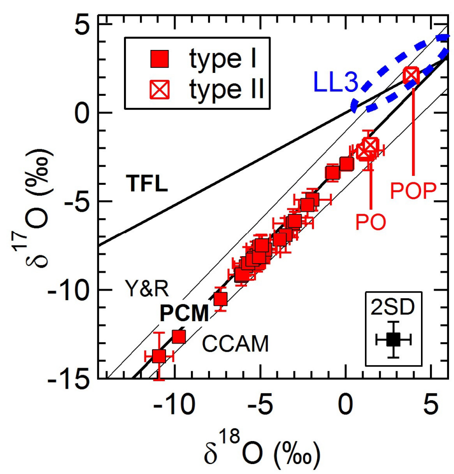

Fig. 1. Oxygen 3-isotope diagram of Y-82094 chondrules. Each datum is the averaged, host value of a chondrule, where uncertainties represent the variability of multiple phenocryst measurements. Dashed oval represents the range of LL3 chondrite chondrule values [6].

chondrules (Fig. 1), consistent with Acfer 094 (ungr. C), CO, CR, and CV chondrite chondrules [10,13-18]. Type II PO and POP chondrules have distinct Δ^{17}O values (–2.6 ‰ to –3.0 ‰ vs. ~+0.1 ‰, respectively); the type II POP chondrules are ~1 ‰ lower in δ^{18}O and ~1 ‰ higher in δ^{17}O, relative to the PCM line. 16 of 35 chondrules have relict olivine and/or spinel grains plotting on/near the PCM line. The percentage of relict-grain-bearing chondrules in Y-82094 is similar to that from Acfer 094, CO, and CV chondrites [10,13,18]. Relict spinels ($n = 2$) are ^{16}O-rich, with Δ^{17}O values of –9.4 ‰ and –19.0 ‰. Relict olivine grains are ^{16}O-rich ($n = 31$) and ^{16}O-poor ($n = 5$) relative to their host chondrule values. 31 of 36 relict olivine grains have Δ^{17}O between –3.8 ‰ and –8.0 ‰, or within the range of host Y-82094 chondrule values, while the remaining five grains are ^{16}O enriched (Δ^{17}O: –10.5 ‰ to –20.6 ‰).

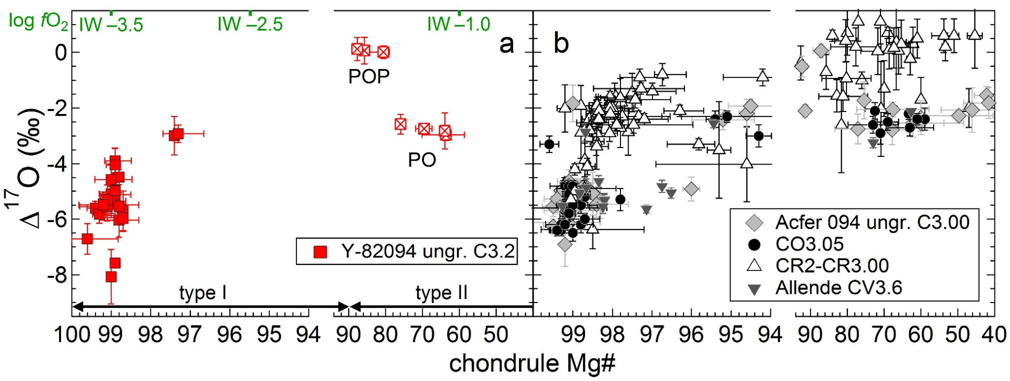

Fig. 2. Comparison of chondrule Mg# versus host Δ^{17}O in Y-82094 (a) and Acfer 094 [10], CO [13], CR [14-17], and CV [18] chondrites (b). Log fO_2 estimates are based on data from [20].

Chondrule $\Delta^{17}O$ vs. Mg#: 25 of 34 chondrules have Mg#'s between 98.7 and 99.6, with host Δ^{17}O values between –3.9 ‰ and –8.1 ‰ (average: –5.5 ‰; Fig. 2a). Two Mg# ~97.3 type I chondrules and the type II PO chondrules (Mg# 63.6 to 75.9) have Δ^{17}O values between –2.6 ‰ and –3.0 ‰. Type II POP chondrules (Δ^{17}O: ~+0.1 ‰) are FeO-poor (Mg#: 80.6 to 87.7) relative to the type II PO chondrules (Fig. 2a).

Mg# ~99 chondrules with Δ^{17}O near –5.5 ‰ are pervasive in Y-82094, Acfer 094, CO, CR, and CV chondrites [10,13-18] (Fig. 2). These are the signatures of a dominant chondrule-forming environment within the carbonaceous chondrite accretion region, especially considering the high percentage of type I chondrules in carbonaceous chondrites (75-99+; e.g. [1-3,19]). According to metal-silicate phase equilibria, this environment existed under highly reducing conditions (log fO_2 – log IW: ~ –3.5; Fig. 2a), equivalent to a CI dust enrichment of ~50× [20]. The increase in Y-82094 chondrule Δ^{17}O with decreasing chondrule Mg# is consistent with chondrules from other carbonaceous chondrites (Fig. 2), supporting the hypothesis [14,17] that addition of relatively ^{16}O-poor H_2O to the highest Mg# chondrule precursors, perhaps through increased dust enrichment [17], contributed to a more oxidized chondrule-forming environment (Fig. 2a). Although rare in Y-82094, type II chondrules sample two distinct O-isotope reservoirs, which could reflect different H_2O amounts and/or different O-isotopes of H_2O in respective environments. The Δ^{17}O –2.6 ‰ to –3.0 ‰ type II PO chondrules are consistent with most CO, Acfer 094, and CV type II chondrules, and some CR type II chondrules (Fig. 2). The Δ^{17}O values of Y-82094 type II POP chondrules (~+0.1 ‰) are similar to some Acfer 094 and CR type II chondrules (Fig. 2), as well as type II chondrules from LL3 chondrites (–0.1 ‰ to +1.2 ‰; [6]), but they differ in δ^{18}O and δ^{17}O (Fig. 3). Finally, Y-82094 type II POP chondrules likely formed at more oxidized conditions than LL3 type I chondrules (e.g. x-axes of Fig. 2a), even though they overlap in δ^{18}O and δ^{17}O (Fig. 3). Therefore, Y-82094 type II POP chondrules likely formed in a different environment than LL3 chondrite chondrules.

References: [1] Kimura M. et al. (2014) *MAPS, 49*, 346-357. [2] Brearley A. J. & Jones R. H. (1998) *Planetary materials*, pp. 3.1-3-398. [3] Weisberg M. K. (2006) *Meteorites and the early solar system II*, pp. 19-52. [4] Rubin A. E. (2010) *GCA*, *74*, 4807-4828. [5] Friedrich J. M. et al. (2015) *Chem. Erde*, doi: 10.1016/j.chemer.2014.08.003. [6] Kita N. T. et al. (2010) *GCA*, *74*, 6610-6635. [7] Yamaguchi A. et al. (2012) *Meteorite Newsletter*, vol. 21, Tokyo: NIPR. [8] Clayton R. N. & Mayeda T. K. (1999) *GCA*, *63*, 2089-2104. [9] Ganguly J. & Tazzoli V. (1994) *Am. Miner.*, *79*, 930-937. [10] Ushikubo T. et al. (2012) *GCA*, *90*, 242-264. [11] Clayton R. N. et al. (1977) *EPSL*, *34*, 209-224. [12] Young E. D. & Russell S. S. (1998) *Science*, *282*, 1874-1877. [13] Tenner T. J. et al. (2013) *GCA*, *102*, 226-245. [14] Connolly, Jr. H. C. & Huss G. R. (2010) *GCA*, *74*, 2473-2483. [15] Schrader D. L. et al. (2013) *GCA*, *101*, 302-327. [16] Schrader D. L. et al. (2014) *GCA*, *132*, 50-74. [17] Tenner T. J. et al. (2015) *GCA*, *148*, 228-250. [18] Rudraswami N. G. et al. (2011) *GCA*, *75*, 7596-7611. [19] Kunihiro T. et al. (2005) *GCA*, *69*, 3831-3840. [20] Ebel D. S. & Grossman L. (2000) *GCA*, *64*, 339-366.

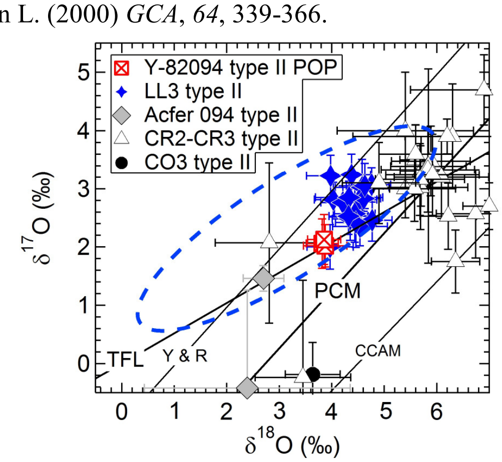

Fig. 3. O 3-isotope plot near LL3 chondrite chondrule data [6]. Dashed oval is the distribution of type I LL3 chondrules.